Optics Letters

Thin active region HgCdTe-based quantum cascade laser with quasi-relativistic dispersion law

A. A. Dubinov,[1,*] D. V. Ushakov,[2] A. A. Afonenko,[2] R. A. Khabibullin,[3,4] M. A. Fadeev,[1] and S. V. Morozov[1]

[1] Institute for Physics of Microstructures, Russian Academy of Sciences, GSP-105, Nizhny Novgorod, 603950, Russia
[2] Belarusian State University, 4 Nezavisimosti Avenue, Minsk, 220030, Belarus
[3] V.G. Mokerov Institute of Ultra-High Frequency Semiconductor Electronics RAS, 7/5 Nagornyy Proezd, Moscow, 117105, Russia
[4] Moscow Institute of Physics and Technology, 9 Institutsky Lane, Dolgoprudny, 141701, Russia
*Corresponding author: sanya@ipmras.ru

Received 18 July 2022; revised 5 September 2022; accepted 5 September 2022; posted 7 September 2022; published 23 September 2022

HgCdTe is promising as a material to solve a problem of the development of semiconductor sources with an operational frequency range of 6–10 THz due to the small optical phonon energies and electron effective mass. In this study, we calculate the dependence of the metal–metal waveguide characteristics on the number of cascades for the 3-well design HgCdTe-based quantum cascade laser at 8.3 THz. It is shown that four cascades are sufficient for lasing at a lattice temperature of 80 K due to the large gain in the active medium. The results of this study provide a way to simplify the fabrication of thin active region HgCdTe-based quantum cascade lasers for operation in the range of the GaAs phonon Reststrahlen band inaccessible to existing quantum cascade lasers.

https://doi.org/10.1364/OL.470688

Currently, quantum cascade laser (QCL) III–V semiconductor-based technology provides a means of producing compact, electrically pumped semiconductor sources of coherent radiation in a large part of terahertz (THz) frequency range [1]. However, the operation of conventional III–V-based QCLs between 6 and 10 THz is complicated by the optical phonon absorption in the Reststrahlen band [2]. Note that, recently, THz QCLs lasing at 8 THz have been designed based on nonpolar (m-plane) GaN quantum wells [3]. It has also been proposed to use ZnO quantum wells [4] and graphene [5] as active media for QCLs in this frequency range due to the high optical phonon energies of these materials. Another advantage of graphene is an electron quasi-relativistic dispersion law, and, as a result, a large gain coefficient [5]. In contrast to III–V semiconductors, II–VI materials, in particular HgCdTe, have lower optical phonon energy, which makes them attractive materials for covering the 6–10-THz gap [6]. HgCdTe is a direct-gap compound semiconductor with a zinc blende crystal structure, in which the bandgap can be varied over a wide range from 0 to 1.6 eV by changing its composition [7]. Recently, thanks to improvements in technology of molecular beam epitaxy growth of HgCdTe structures with narrow-gap quantum wells (QWs), with the quasi-relativistic dispersion law, it became possible to grow a waveguide structure with 15 QWs and demonstrate interband stimulated emission with a frequency of 9.7 THz under optical pumping [8]. Furthermore, the possibility of THz operation of different devices with multiple QWs based on HgCdTe was shown theoretically. These include a bipolar laser diode for the frequency range of 10–11.5 THz [9] and a QCL emitting at 8.3 THz [10].

It should be noted that both variants of electrically pumped lasers proposed in Refs. [9] and [10] might face serious difficulties with practical implementation. For laser structures with a *p*-*n* junction, the main obstacle is the formation of a *p*-type layer. To activate the acceptors, it requires thermal annealing, which interferes with the growth of high-quality QWs [11]. Such a problem is not present for unipolar QCLs. However, unlike conventional bipolar semiconductor lasers with only a few QWs, QCL devices typically contain laser active regions (ARs) that are several microns thick and comprise several hundred nanometer-scale semiconductor layers of precisely controlled thicknesses and compositions.

The use of a metal–metal waveguide for terahertz QCLs based on GaAs allows a considerable reduction of the required AR thickness. For example, for a 3.5-THz laser, it was possible to reduce the AR thickness down to 1.75 µm [12], which is 50 times smaller than the wavelength of the laser in vacuum. The AR was based on a three-well resonant-phonon design and consisted of just 37 cascades each with a 43.7 nm thickness. In addition, thanks to reduced heat dissipation and lower thermal resistance, the thinner AR shows an increase in the continuous wave operating temperature compared to the thicker AR [13]. The gain, g, in THz QCLs based on HgCdTe QWs in the temperature range of up to 150 K is several times larger than in THz QCLs based on GaAs [10]. The advantage of HgCdTe-based QCLs over GaAs-based QCLs is due to the much lower effective mass of electrons (due to quasi-relativistic dispersion law), m, in HgCdTe QWs, which results in higher gain ($g \sim m^{-3/2}$) [14] (Fig. 1). For example, in the $Hg_{0.8}Cd_{0.2}Te/Hg_{0.6}Cd_{0.4}Te$ QW, $m = 0.03m_0$, where m_0 is the free-electron mass, while in $GaAs/Al_{0.15}Ga_{0.85}As$ QWs, $m = 0.067m_0$. Thus, there is a possibility to further decrease the number of cascades of the laser and overall AR thickness, which should facilitate its development.

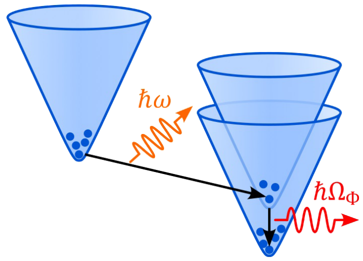

Fig. 1. Schematic description of the relevant subbands and transitions with photon (hω) and phonon ($h\Omega_\Phi$) emission in a HgCdTe-based quantum cascade laser.

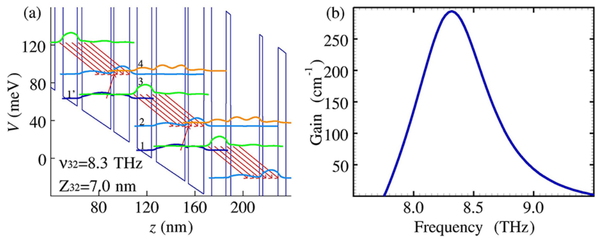

Fig. 2. (a) Conduction band profile and associated square-wave functions, calculated within the kp-method, for an optimized 8.3-THz QCL with three $Hg_{0.8}Cd_{0.2}Te/Hg_{0.6}Cd_{0.4}Te$ QWs. The voltage on one cascade is equal to 55 mV, temperature $T = 77$ K. The red arrows indicate the main current channels through the structure. (b) Gain spectrum of the AR with three $Hg_{0.8}Cd_{0.2}Te/Hg_{0.6}Cd_{0.4}Te$ QWs.

In this Letter, we carry out a theoretical investigation of the possibility to reduce the number of cascades (AR thickness) in THz QCLs based on HgCdTe QWs.

In our calculations, we consider the 3-well design QCL. The layer sequence of the single period of such design in nanometers is **6.5**/11.7/**3.9**/24.0/**2.6**/13.0 with $Hg_{0.6}Cd_{0.4}Te$ barriers indicated in bold letters, where the central part of underlined $Hg_{0.8}Cd_{0.2}Te$ well is doped with a sheet electron density of $6.2 \times 10^{10}\,cm^{-2}$. We consider 50-nm-thick n^+-CdTe contact layers with a doping concentration of $10^{17}\,cm^{-3}$. Figure 2(a) shows the calculations of quantization levels and wave functions for the considered structure. The levels in the cascade are numerated as 1–4 from bottom to top. Injection of electrons to the upper laser level 3, is achieved by resonant tunneling from the main level 1' of the broad well of the previous cascade. Electrons then transition radiatively to a lower laser level 2, which is effectively emptied by non-radiative transition to level 1 by emission of an optical phonon. Level 4 serves for more effective emptying of the lower laser level of the previous cascade and extending the positive part of volt-ampere characteristic. Diagonal laser transition (3–2) with dipole matrix element $Z_{32} = 7.0$ nm is realized at the frequency of 8.3 THz and corresponds to the maximum of the gain spectrum. The matrix element which is two times higher (in comparison with GaAs-based QCLs) provides a large gain of $300\,cm^{-1}$ [Fig. 2(b)]. The details of the calculation method are given in Ref. [10].

To calculate the dependence of dielectric permittivity of n^+-CdTe on cycle frequency ω, we used the following expression:

$$\varepsilon_1(\omega) = \varepsilon_1^*(\omega) - \frac{\omega_1^2}{\omega^2 + i\gamma_1\omega}, \tag{1}$$

where $\varepsilon_1^*(\omega)$ is the dielectric permittivity of undoped CdTe [15], $\gamma_1 = q/(m_1\mu_1)$, q is the elementary charge, and $\omega_1^2 = 4\pi N_1 q^2/m_1$, μ_1, m_1, and N_1 are the square of plasma frequency, mobility, effective mass, and concentration of electrons in n^+-CdTe, respectively.

The mobility of electrons in n^+-CdTe at a temperature around 80 K and electron concentration of $10^{17}\,cm^{-3}$ can be considered to be $10^3\,cm^2/(V\cdot c)$ [16] and the effective mass to be $m_1 = 0.095 m_0$ [17]. For calculating the frequency dependence of the dielectric permittivity of the AR, we used following approximation (accounting for the thickness of one cascade being much less than the wavelength of radiation in the AR):

$$\varepsilon_2(\omega) = \frac{\varepsilon_{2,1}(\omega)d_1 + \varepsilon_{2,2}(\omega)d_2}{d_1 + d_2}, \tag{2}$$

where $\varepsilon_{2,1}(\omega)$ and d_1 are respectively the dielectric permittivity and total thickness of $Hg_{0.6}Cd_{0.4}Te$ barriers in one cascade; $\varepsilon_{2,2}(\omega)$ and d_2 are respectively the dielectric permittivity and total thickness of $Hg_{0.8}Cd_{0.2}Te$ QWs in one cascade.

The formula for the frequency dependence of the dielectric permittivity of $Hg_{0.6}Cd_{0.4}Te$ ($n = 1$) and $Hg_{0.8}Cd_{0.2}Te$ ($n = 2$) was approximated within the multioscillator model from the experimental data:

$$\varepsilon_{2,n}(\omega) = \varepsilon_{\infty,n} + \sum_{j_n} \frac{S_{j_n}\omega_{TO,j_n}^2}{\omega_{TO,j_n}^2 - \omega^2 - i\omega\gamma_{j_n}} - \frac{\omega_2^2}{\omega^2 + i\gamma_2\omega}\delta_{2,n}, \tag{3}$$

where $\delta_{2,n}$ is the Kronecker delta, $\varepsilon_{\infty,n}$ is the high frequency dielectric constant, and S_{j_n}, ω_{TO,j_n}, and γ_{j_n} represent the strength, frequency, and damping constant for the jth oscillator and nth semiconductor. These parameters were taken from the works of [18] and [19] for $Hg_{0.6}Cd_{0.4}Te$ and $Hg_{0.8}Cd_{0.2}Te$, respectively. When calculating plasma frequency ω_2 and damping constant γ_2, we used the following values: the concentration and mobility of electrons in $Hg_{0.8}Cd_{0.2}Te$ were equal to $10^{16}\,cm^{-3}$ and $10^5\,cm^2/(V\cdot c)$, respectively [20]. Dielectric permittivity of silver $\varepsilon_m(\omega)$ (the metal, which can be used for the fabrication of the metal–metal waveguide) was determined from the Drude model, the parameters for which were experimentally found in a previous work [21].

The coordinate dependence of the module of the magnetic field $H_y(z)$ of the TM mode of the QCL propagating along the x axis (z axis points in the growth direction) is found from the following equation [22]:

$$\varepsilon(z,\omega)\frac{d}{dz}\left[\frac{1}{\varepsilon(z,\omega)}\frac{dH_y(z)}{dz}\right] + \left(\varepsilon(z,\omega)\frac{\omega^2}{c^2} - k_x^2\right)H_y(z) = 0, \tag{4}$$

where c is the speed of light in vacuum, $k_x = n_{ef}\omega/c$ is the longitudinal component of the wave vector of the mode, and n_{ef} is effective refractive index of the mode. The distribution of dielectric permittivity is expressed as

$$\varepsilon(z,\omega) = \begin{cases} \varepsilon_m(\omega), z<0, z \geq 2d + N(d_1+d_2) \\ \varepsilon_1(\omega), 0 \leq z<d, d+N(d_1+d_2) \leq z<2d+N(d_1+d_2) \\ \varepsilon_2(\omega), d \leq z<d+N(d_1+d_2) \end{cases}, \tag{5}$$

where N is the number of cascades in the QCL under consideration and d is the contact layer thickness. Here, $H_y(z)$ and $\frac{1}{\varepsilon(z,\omega)}\frac{dH_y(z)}{dz}$ are continual on the boundary between layers with different permittivity. Additionally, $H_y(z) \to 0$ at $z \to 0$ is a boundary condition for the waveguide mode. The component

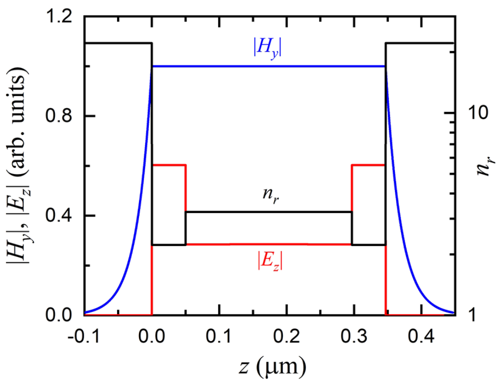

Fig. 3. Spatial distribution of $|H_y|$, $|E_z|$, and n_r in the waveguide of the considered QCL with $N = 4$.

of the electric field of the TM mode $E_z(z)$ is found from the equation:

$$E_z(z) = -\frac{ck_x}{\omega\varepsilon(z,\omega)}H_y(z). \quad (6)$$

The spatial distribution of the calculated $|H_y(z)|$, $|E_z(z)|$, $|E_x(z)|$, and $n_r = Re(\sqrt{\varepsilon(z,\omega)})$ in the waveguide of the considered QCL with $N = 4$ is shown in Fig. 3.

To find the minimal possible number of cascades in the considered QCL, we used an expression for determining the threshold of generation [22]:

$$g\Gamma = \alpha_{in} + \alpha_m, \quad (7)$$

where $\alpha_m = -\ln(R)/L$ is the loss coefficient on the mirrors of the laser with length L and the reflection coefficient on a mirror R, $\alpha_{in} = 2\text{Im}(k_x)$ represents the internal optical losses in the waveguide of the laser, and Γ is the optical confinement factor of the TM mode [23]:

$$\Gamma = \frac{Re(n_{ef}) \int_{d}^{d+N(d_1+d_2)} n_r|E_z(z)|^2 dz}{\int_{-\infty}^{+\infty} n_r^2|E_z(z)|^2 dz}. \quad (8)$$

Note that it is possible to use a simpler expression for obtaining Γ, without calculating the distribution of electromagnetic fields from Eqs. (4), (6) and the integrals in Eq. (8), which provides the same result:

$$\Gamma = \frac{\partial Re(n_{ef})}{\partial n_r}. \quad (9)$$

As it is known, the losses on the mirrors of the THz QCLs with a thin metal–metal waveguide are small [24]. An estimate for α_m for $L = 1$ mm and $R \sim 0.9$ [24] gives the value of approximately 1 cm^{-1}. Internal losses for thin waveguides are larger and can be calculated (so as Γ) from Eqs. (4), (6), and (8).

Figure 4(a) shows the calculated frequency dependence of the optical confinement factor for several values of the number of cascades in the AR. The confinement factor weakly depends on the temperature and frequency in the GaAs phonon Reststrahlen band, but significantly changes with the number of cascades. At a frequency of 8.3 THz, it is equal to 0.31, 0.48, 0.59, 0.67, and 0.72 for 2, 4, 6, 8, and 10 cascades, respectively.

Figure 4(b) shows the temperature dependence of total losses and modal gain $g\Gamma$ for several values of the number of cascades in the considered QCL. The dependence of losses on temperature is associated with a decrease in the conductivity of metal plates [21] and the mobility of electrons in semiconductor layers [7] with increasing temperature. As one can see, four periods of the QCL are already enough for obtaining generation with a maximum operating temperature of 80 K. When increasing the number of periods from 4 to 10, the operating temperature increases up to 107 K. This fact is explained by the decrease of the loss coefficient and the increase of the optical confinement factor, which overcome the decrease of the amplification coefficient with temperature. Consequently, one can assume that with the given parameters of QCL structure, four cascades are enough for the generation. Each cascade consists of three quantum wells and has the thickness of 61.7 nm, thus the total waveguide thickness of such a QCL is 104 times smaller than the wavelength of the laser in vacuum.

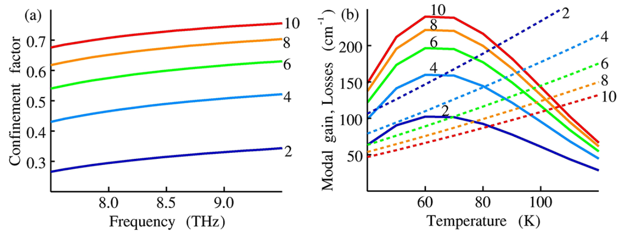

Fig. 4. (a) Spectral dependence of the optical confinement factor for different numbers of cascades (numbers next to the curves); $T = 77$ K. (b) Temperature dependencies of modal gain coefficient (solid curves) and corresponding loss coefficients (dashed curves) at 8.3-THz frequency for different numbers of cascades (numbers on the curves).

In conclusion, we performed modeling of the waveguide characteristics of an HgCdTe-based 8.3-THz QCL with 3-well design of a cascade [10] and metal–metal waveguide. The results show that four cascades are enough for the operation of such a laser at a temperature of 80 K. The total thickness of the waveguide is equal to $d_w = 347$ nm, making the ratio between the wavelength and waveguide thickness, λ/d_w, two times larger than the record result reported earlier for a THz QCL based on GaAs [12]. Such a small thickness of the AR of the HgCdTe-based QCL is reached thanks to the amplification coefficient which is several times larger than for GaAs-based THz QCLs due to quasi-relativistic dispersion law of HgCdTe QWs. Predicted characteristics make the growth of QCLs based on HgCdTe QWs for the frequency gap of 6–10 THz significantly more accessible.

Funding. Ministry of Science and Higher Education of the Russian Federation (075-15-2020-797 (13.1902.21.0024)).

Acknowledgments. Authors thanks Dr. Maxim Zholudev for his help in preparing the article.

Disclosures. The authors declare no conflicts of interest.

Data availability. Data underlying the results presented in this paper are not publicly available at this time but may be obtained from the authors upon reasonable request.

REFERENCES

1. M. S. Vitiello, G. Scalari, B. Williams, and P. D. Natale, Opt. Express **23**, 5167 (2015).
2. K. Feng, W. Streyer, Y. Zhong, A. Hoffman, and D. Wasserman, Opt. Express **23**, A1418 (2015).
3. L. Wang, T.-T. Lin, M.-X. Chen, K. Wang, and H. Hirayama, Appl. Phys. Express **14**, 112003 (2021).
4. V. P. Sirkeli and H. L. Hartnagel, Opto-Electron. Rev. **27**, 119 (2019).

5. A. A. Dubinov, A. Bylinkin, V. Ya. Aleshkin, V. Ryzhii, T. Otsuji, and D. Svintsov, Opt. Express **24**, 29603 (2016).
6. S. Ruffenach, A. Kadykov, V. V. Rumyantsev, J. Torres, D. Coquillat, D. But, S. S. Krishtopenko, C. Consejo, W. Knap, S. Winnerl, M. Helm, M. A. Fadeev, N. N. Mikhailov, S. A. Dvoretskii, V. I. Gavrilenko, S. V. Morozov, and F. Teppe, APL Mater. **5**, 035503 (2017).
7. A. Rogalski, Rep. Prog. Phys. **68**, 2267 (2005).
8. S. V. Morozov, V. V. Rumyantsev, M. S. Zholudev, A. A. Dubinov, V. Ya. Aleshkin, V. V. Utochkin, M. A. Fadeev, K. E. Kudryavtsev, N. N. Mikhailov, S. A. Dvoretskii, V. I. Gavrilenko, and F. Teppe, ACS Photonics **8**, 3526 (2021).
9. A. Afonenko, D. Ushakov, G. Alymov, A. Dubinov, S. Morozov, V. Gavrilenko, and D. Svintsov, J. Phys. D: Appl. Phys. **54**, 175108 (2021).
10. D. Ushakov, A. Afonenko, R. Khabibullin, D. Ponomarev, V. Aleshkin, S. Morozov, and A. Dubinov, Opt. Express **28**, 25371 (2020).
11. S. A. Dvoretsky, N. N. Mikhailov, V. G. Remesnik, Yu. G. Sidorov, V. A. Shvets, D. G. Ikusov, V. S. Varavin, M. V. Yakushev, J. V. Gumenjuk-Sichevska, A. G. Golenkov, I. O. Lysiuk, Z. F. Tsybrii, A. V. Shevchik-Shekera, F. F. Sizov, A. V. Latyshev, and A. L. Aseev, Opto-Electron. Rev. **27**, 282 (2019).
12. E. Strupiechonski, D. Grassani, D. Fowler, F. H. Julien, S. P. Khanna, L. Li, E. H. Linfield, A. G. Davies, A. B. Krysa, and R. Colombelli, Appl. Phys. Lett. **98**, 101101 (2011).
13. C. A. Curwen, S. J. Addamane, J. L. Reno, M. Shahili, J. H. Kawamura, R. M. Briggs, B. S. Karasik, and B. S. Williams, AIP Adv. **11**, 125018 (2021).
14. E. Benveniste, A. Vasanelli, A. Delteil, J. Devenson, R. Teissier, A. Baranov, A. M. Andrews, G. Strasser, I. Sagnes, and C. Sirtori, Appl. Phys. Lett. **93**, 131108 (2008).
15. E. D. Palik, *Handbook of Optical Constants of Solids* (Academic Press, 1985).
16. F. Bassani, S. Tatarenko, K. Saminadayar, N. Magnea, R. T. Cox, A. Tardot, and C. Grattepain, J. Appl. Phys. **72**, 2927 (1992).
17. O. Madelung, *Semiconductors: Data Handbook* (Springer-Verlag, 2003).
18. J. H. Chu and S. C. Shen, Semicond. Sci. Technol. **8**, S86 (1993).
19. Q. Dingrong, J. Appl. Phys. **70**, 7191 (1991).
20. S. Krishnamurthy and A. Sher, J. Appl. Phys. **75**, 7904 (1994).
21. D. V. Ushakov, A. A. Afonenko, A. A. Dubinov, V. I. Gavrilenko, I. S. Vasil'evskii, N. V. Shchavruk, D. S. Ponomarev, and R. A. Khabibullin, Quantum Electron. **48**, 1005 (2018).
22. H.C. Casey and M.B. Panich, *Heterostructure Lasers* (Academic Press, 1978).
23. Y.-Z. Huang, Z. Pan, and R.-H. Wu, J. Appl. Phys. **79**, 3827 (1996).
24. S. Kohen, B. S. Williams, and Q. Hu, J. Appl. Phys. **97**, 053106 (2005).